Reinventing Space Conference
RS-2011-4004

Space Rapid Transit for Rapid Spacecraft Deployment

Paul R. Griesemer
Princeton Satellite Systems, Inc.

Michael A. Paluszek
Princeton Satellite Systems, Inc.

Joseph B. Mueller
Princeton Satellite Systems, Inc.

Eloisa de Castro
Princeton Satellite Systems, Inc.

Reinventing Space Conference
May 2 – 6, 2011
Los Angeles, CA

AIAA-RS-2011-4004

Space Rapid Transit for Rapid Spacecraft Deployment

Paul R. Griesemer, Michael A. Paluszek, Joseph B. Mueller, Eloisa de Castro
pgriesemer, map, jmueller, edecastro @psatellite.com
Princeton Satellite Systems, Inc.
6 Market Street, Plainsboro, NJ 08536
609-275-9606

In the past several years, technological advances in fields such as lightweight structures, propulsion and thermal protection systems have made the oft-studied concept of a two-stage-to-orbit (TSTO), horizontally launched, horizontally landed reusable launch vehicle increasingly achievable at a relatively low development risk. Princeton Satellite Systems is developing the Space Rapid Transit (SRT) small satellite launch vehicle to address the most critical needs of the United States space program: namely the rapid, safe and economic delivery of payloads and astronauts into low Earth orbit. Potential missions are ISS resupply, small satellite deployment, high altitude reconnaissance, and even ISS astronaut emergency return to earth.

The SRT Ferry stage is a waverider design powered by a combined cycle engine, which can operate as 1) a turbofan, 2) a turbofan in parallel with a ramjet and 3) as a ramjet. The SRT Upper stage is a lifting body configuration similar to the Space Shuttle, and uses a RL 10B-2 engine for orbit insertion. Many aspects of the SRT are designed to reduce operational costs – the core avionics system is identical for both stages and based on the Boeing 787 system; the two stages mate automatically with no need for additional mechanisms; and the use of a new "green propellant" eliminates the handling of toxic hydrazine. Discussions with potential engine subcontractors indicate that first test flights could be conducted within 3 years after the beginning of Phase C. The design of the SRT permits a phased development program with independent testing of the Ferry and Upper Stages. The Ferry Stage can be tested using a turbofan engine alone prior to integration of the combined cycle engine.

This paper presents the system design of the SRT and provides additional details of its GN&C system during all phases of operations. Aerodynamic models and mass budgets are presented, along with a discussion of the reentry profile.

KEYWORDS: air launch, two stage to orbit, launch vehicle, hypersonic, combined-cycle engine, guidance, control

Introduction

Two of the major challenges facing the United States space program today are to bring time-critical payloads into low-earth orbit and to bring astronauts into orbit safely and economically. Princeton Satellite Systems is designing the SRT to solve these problems.

The SRT is a class of horizontally-launched, horizontally landing fully reusable two-stage to orbit vehicle. This concept is not new and was the basis for the German Saenger and NASA Beta concepts. SRT is designed to bring 425 kg payloads to the International Space Station. This would fully test the SRT concept and provide the U.S. with a responsive launch vehicle.

The Ferry Stage accelerates to M = 4.6 at which point the Upper Stage ignites its RL 10B-2 engine. Two burns bring the Upper Stage into a circular orbit. On orbit control is performed with the ECAPS High Performance Green Propellant (HPGP) Thrusters recently tested on the PRISMA mission. The Ferry Stage glides to subsonic speeds and then restarts the turbofan for powered landing. The Upper Stage deorbit burn uses the HPGP thrusters and it glides to reentry. The Upper Stage is similar in configuration to the Space Shuttle. Optimal trajectory studies show that an F-22 sized SRT can bring 425 kg to the ISS.

The SRT design implements many features to reduce operational costs. The HPGP thrusters and auxiliary power unit (APU)eliminate the handling of toxic hydrazine. The core avionics system on the Upper and Ferry Stages is identical and based on the Boeing 787 system for integration into commercial air space, a requirement at least for abort landings. The flight software on both Stages is identical and either can be used to fly the entire vehicle. The Ferry and Upper Stage mate automatically without any additional fixtures or mechanisms. The SRT is fully reusable although the RL 10B-2 engine would need to be replaced every 6 to 7 flights.

The SRT requires guidance and control systems for each phase of operation of both stages. The Upper Stage is similar conceptually to the Space Shuttle Orbiter and the Ferry Stage is similar to a supersonic fighter. However, both are remotely piloted. Because the SRT is designed for launch at from any airport it must work with the existing air traffic control system.

This paper discusses the overall design of the vehicle and updates simulation results from take off to landing of both stages. Two vehicle designs are presented.

Concept of Operations

Introduction

SRT allows for rapid launch of satellites from any location on earth. Any airfield becomes a launch site. The only requirement is a supply of liquid hydrogen and oxygen for the Upper Stage. Some of the unique capabilities are discussed in this section. An ISS resupply mission is shown in Figure 2.

On-Demand Imaging, SIGINT or Communications Mission

On-demand imaging, SIGINT or communications involves the rapid insertion of a satellite into orbit, with a ground-track designed to support military operations. The satellite remains in orbit permanently. An advantage of on-demand satellites is that the payload can be added at the last minute thus taking advantage of the latest technology or having capabilities customized to the mission.

Reconstitution of a Satellite Constellation

SRT can add new satellites to an existing satellite constellation. A vehicle such as the SRT has the advantage of a low turn-around time, so it may be possible to rapidly launch several payloads with a single vehicle, or a single Ferry Stage with multiple Upper Stages. This eliminates the need for spares in constellations thus lowering costs.

Mission Specific Reusable Satellites and Satellite Recovery

A reusable satellite could be created that is intended for a limited duration mission. The satellite is released from the SRT, completes its mission, and then is recaptured and reused at a later date. The re-use of the satellite could reduce the overall program costs and enable the creation of a new class of small satellites that are highly specialized for specific activities. Since the satellites would not need to operate for long periods of time they would not need to have extensive redundancy. In addition, if one failed a new one could be launched.

SRT as a Sensor Platform

SRT can serve as a reusable sensor platform itself. This is much like the recent X-37B mis-

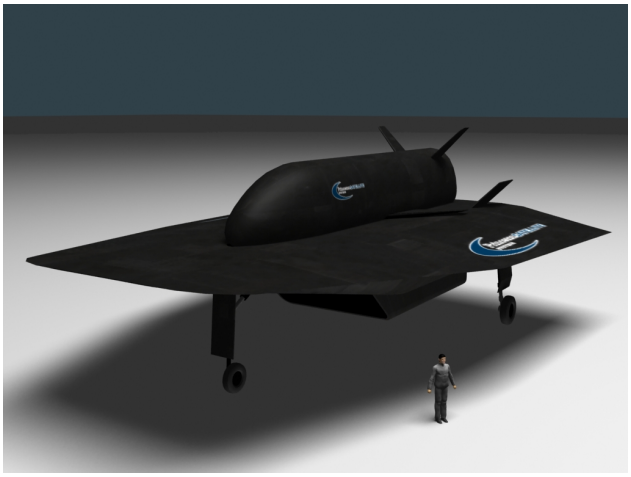

Figure 1: **SRT**

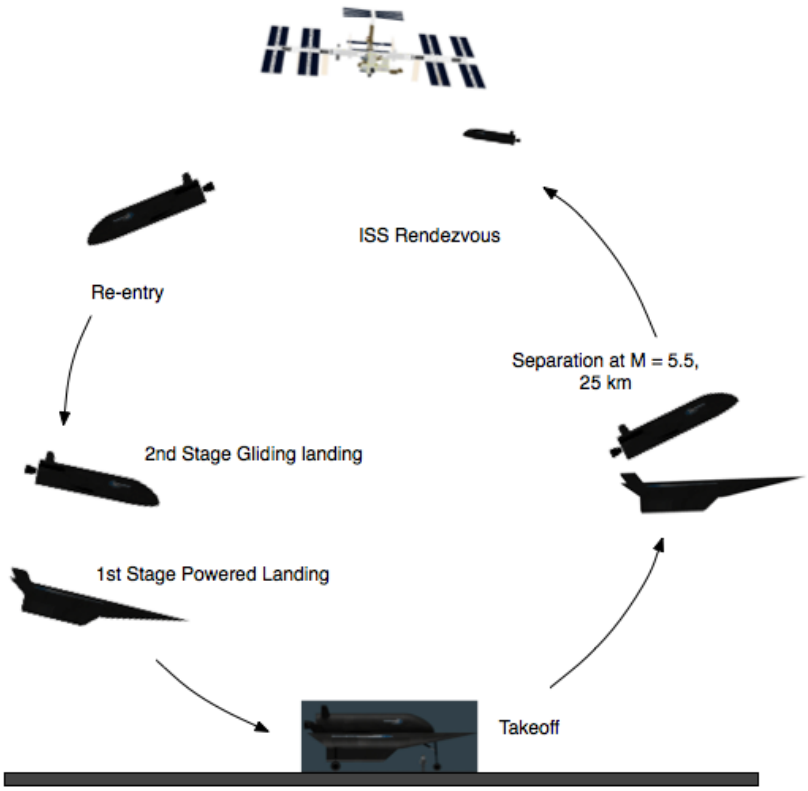

Figure 2: **Mission sequence**

sion. An SRT can be launched on demand from an airfield and can then either perform a single suborbital pass over a target or go into a low earth orbit. This allows commanders to get intelligence information quickly and prevents an adversary from responding to the mission since the adversary could not know the orbit.

Vehicle Design Overview

Introduction

The SRT system is designed to fully utilize available technology and produce a low-risk development plan.[1] The SRT ferry stage uses conventional military turbofan engines using jet fuel to reach Mach 1.5. At that point a hydrogen fueled ramjet propels the vehicle to Mach 5.5 at an altitude of 25 km. Dual fuel permits the ferry stage to easily move the SRT between airfields. Stage separation occurs and a liquid oxygen/liquid hydrogen rocket engine based on the Pratt & Whitney RL-60 takes the orbiter into earth orbit. The SRT Ferry stage is roughly F-22 sized and the SRT orbiter is similar to the NASA/DARPA/Air Force X-37B. A hydrogen fueled ramjet was tested by MBB as part of the German Saenger program. The reaction control system on the second stage would use the Swedish Space Corporation's HPGP Thruster which uses a green propellant. This would simplify ground operations by eliminating the handling of toxic hydrazine. The orbiter attaches below the ferry stage for ease of ground integration. Both have undercarriages so integration on the ground is simply a matter of rolling the orbiter under the ferry stage.

Different views of the vehicle and its stages are shown in Figure 3. The design of the Ferry Stage is a compromise between subsonic ferry performance and performance at high Mach numbers during the launch trajectory. It is expected that this will change as structural, thermal and propulsion analyses are performed and the design is refined. It is worth noting that the X-15 covered a similar range of Mach and altitude as the SRT Ferry Stage.

Guidance and Control

The two vehicles, the Ferry Stage and Upper Stage, have independent control systems. The Upper Stage operates after separation. The Ferry Stage system is basically a high-speed aircraft control system. It operates in all flight regimes from takeoff through separation and back to landing. It is fully autonomous but allows for operators on the ground to override the automatic systems. The unified control system is shown in Figure 4. Both vehicles fly exactly the same flight software and either vehicle can control the other providing an additional level of redundancy.

Pilot control of the vehicles is from the ground for SRT-M and from the Upper Stage or the ground in SRT-C. This is shown if Figure 5. The crew stations onboard SRT-C are identical to the crew stations on the ground. Although the ground control stations are nominally Ferry and Upper Stage either can control either vehicle.

Propulsion

Upper Stage Main Propulsion

The upper stage engine is the Pratt & Whitney RL10B-2 rocket engine.[2–4] A feature of the RL10B-2 model is its large carbon-carbon composite translating nozzle extension which adds 30 seconds of specific impulse over the base 77:1 expansion ratio. The combination of starts and burn time would potentially permit the engine to be used on up to five flights before it would need to be replaced. Table 1 shows the parameters of the RL10B-2 engine.

Table 1: RL-10B-2

Parameter	Value
Thrust	110.1 kN
Burn Time	1152 sec
Starts	15
Mass	277 kg
Specific Impulse	465 sec
Gimbal Range	4 deg

Figure 3: SRT stages

1. Upper Stage Reaction Control System

Figure 6 shows the Reaction Control System. The system is a blowdown pressurization system with two tanks which can feed any bank of 8 thrusters and 1 APU. The thrusters are fully cross strapped.

ECAPS thrusters are the baseline reaction control system engine for the Upper Stage.[5] Parameters are given in Table 2 and the engine is shown in Figure 6. The 1 N HPGP engines are currently flying onboard the Swedish Space Corporation's PRISMA spacecraft. The HPGP engines use a non-toxic propellant thus greatly simplifying ground operations. 22 N thrusters are available and larger thrusters are planned.

Table 2: HPGP Engines

Parameter	Value
Propellant	LMP-103S
Inlet Pressure Range	5 - 25 bar
Thrust Range vacuum	5 - 22 N
Isp vacuum	2200 - 2400 Ns/kg
Density Impulse vacuum	2700 - 2975 Ns/L
Rise Time to 90% thrust	50 ms
Decay Time to 10% thrust	$<$ 300 ms
Valve Heater Power	Mission Specific
Overall Length	216 mm
Mass	0.75 kg

Ferry Stage Combined Cycle Engine

The combined cycle engine is shown in Figure 7.

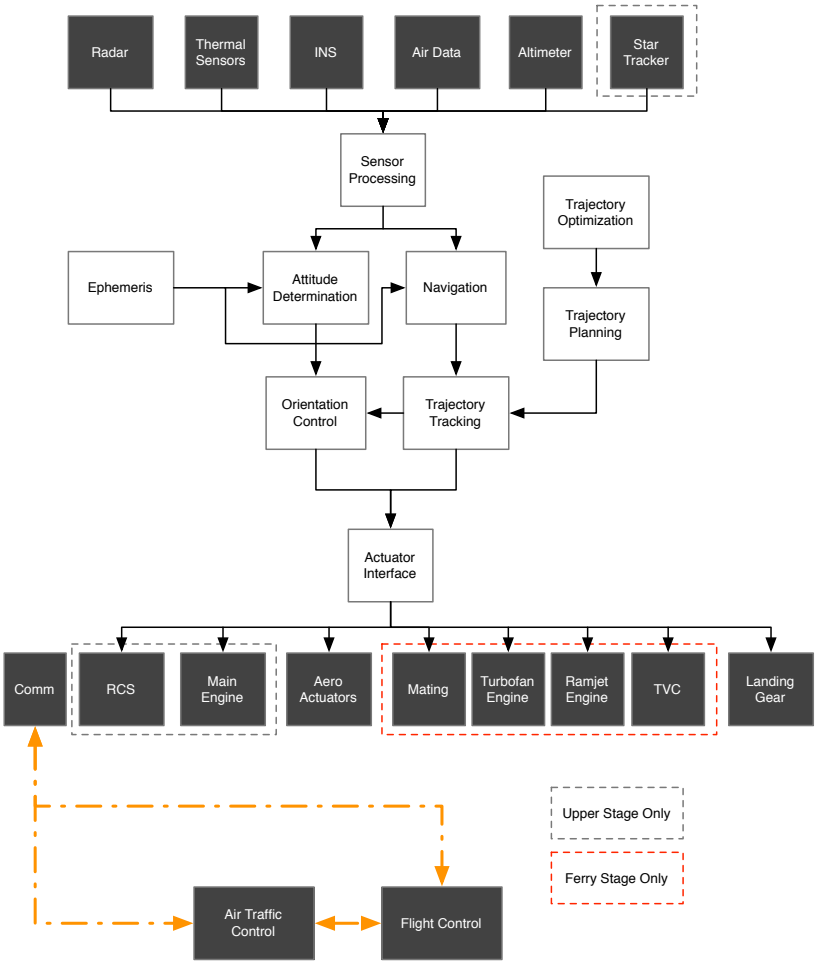

Figure 4: Unified control architecture

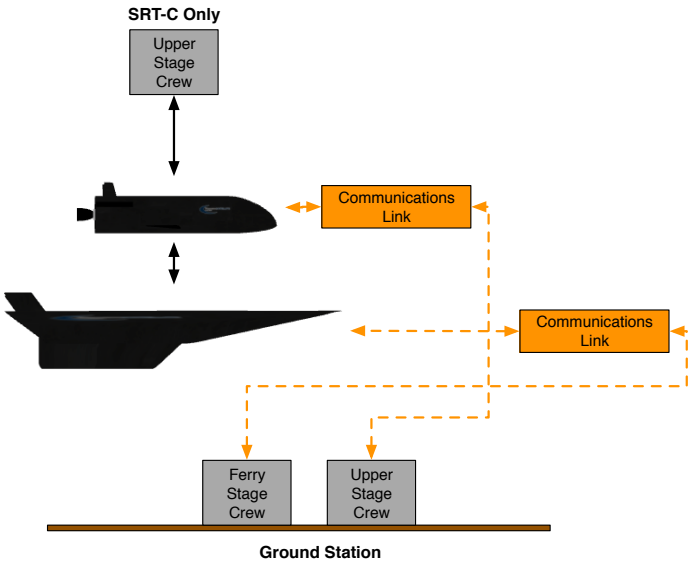

Figure 5: Crew control

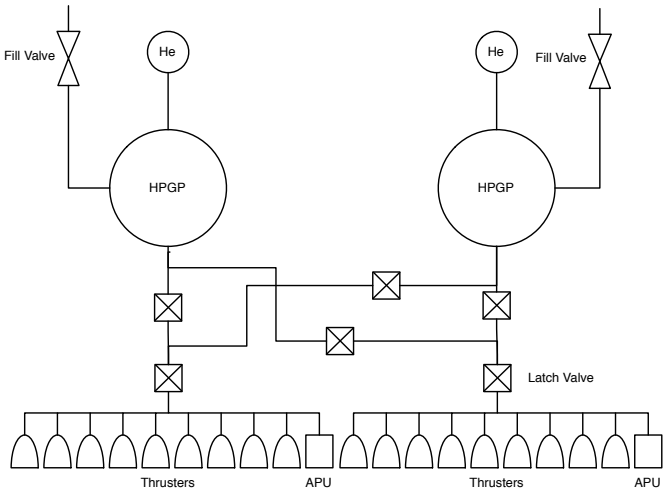

(a) Schematic

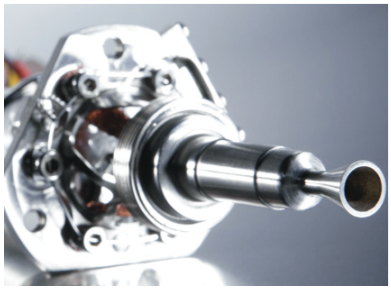

(b) ECAPS 5 N Engine

Figure 6: RCS system

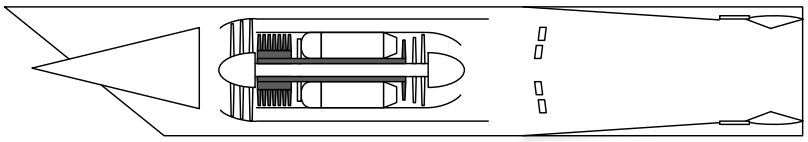

Figure 7: **Coaxial Dual Fuel Ramjet**

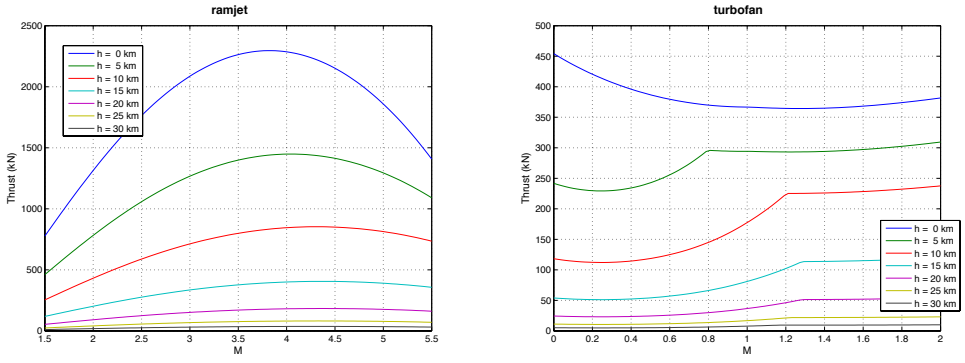

Figure 8: **Engine performance**

Cryogenic Tanks

Structural Mechanisms

Prior to launch, the SRT Upper Stage is top-mounted to the Ferry Stage using a complete mating system requiring no external equipment. This setup is advantageous in that aerodynamic degradation is low, vehicles may launch from any airfield and time-to-launch is significantly reduced. A diagram of the process is shown in Figure 9. The loading sequence is as follows:

1. Ferry Stage kneels on front landing gear
2. Unfueled Upper Stage is rolled onto the Ferry Stage
3. Upper Stage gear retracts
4. Latches are locked
5. Ferry stage rises
6. Both vehicles are fueled

The Ferry Stage lowers itself at the nose and the Upper Stage is pulled atop. The SRT nose landing gear deviates from already-existent landing gear designs in that in addition to its fully extended and fully retracted states, it is designed with a third "kneeling" or transitional retraction configuration. It is weight bearing both when it is extended and kneeling. The three arrangements are illustrated in Figure 10.

Avionics

The avionics is discussed in.[6] Both stages use the same core avionics, based on the Boeing 787, for atmospheric flight. The Upper Stage has additional hardware for in-orbit operations and control of the RCS and main engine. The Ferry Stage has additional hardware for combined-cycle engine control. Both vehicles are designed for integration into the air traffic control system. Even if they are launched from restricted air space it may be necessary during an abort to land the vehicles at an airport in unrestricted air space.

Mass Statements

The and Ferry Stage group mass statement is given in Table 3.

Table 3: SRT Ferry Stage Group Mass Statement

Item	Group	Mass	Percentage
1	fuselage	1318	4.69
2	wing	1238	4.406
3	nacelle	1545	5.499
4	undercarriage	1236	4.4
5	misc	0	0
6	power plant	4763	16.95
7	systems	3091	11
8	furnishings	1826	6.5
9	contingency	421.5	1.5
10	crew	0	0
11	payload	9463	33.68
12	fuel	3196	11.37
	Total	28097.6	100.00

The Upper Stage group mass statement is given in Table 4

Table 4: SRT Upper Stage Group Mass Statement

Item	Group	Mass	Percentage
1	fuselage	1134	7.84
2	wing	202.7	1.401
3	empennage vertical	72.36	0.5002
4	undercarriage	636.5	4.4
5	misc	0	0
6	power plant	1551	10.72
7	systems	1591	11
8	furnishings	940.2	6.5
9	contingency	217	1.5
10	crew	0	0
11	payload	425	2.938
12	fuel	7695	53.2
	Total	14465.2	100.00

Control

The SRT has both manual control and automatic control. All operations from launch

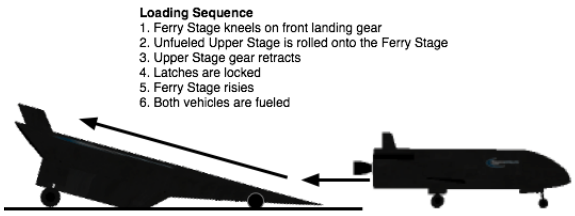

Figure 9: SRT Stage Mating Process

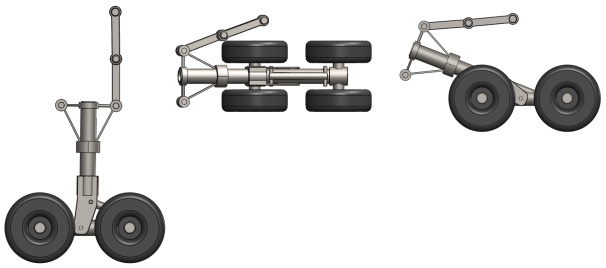

Figure 10: Kneeling Nose Gear Configurations

through landing of both stages can be done autonomously. However, both vehicles can be remote piloted. The control consoles are on the ground but a second console for the Upper Stage would be onboard the ISS. Figure 16 shows the control layout. The Upper Stage has two joysticks, one for translation and one for rotation. Both joysticks have 3 degrees-of-freedom. Rotation modes are angular increment, rate increment, pulse and continuous thrust. Angular increment and rate are actually commands to the automatic attitude control system. Attitude control can be performed in the Upper Stage with the RCS system, aerodynamic actuators or a blend of both. During main engine burn the gimbal angles of the main engine are used for yaw and pitch control. The Ferry Stage blends thrust vector control with aerodynamic control.

Simulations Models and Flight Software

Introduction

A detailed closed-loop simulation has been developed to help design and validate the guidance laws. The SRT ferry and upper stages are modeled as independent 6 degree of freedom bodies, with the upper stage kinematically constrained to the ferry stage during mated flight.

A. Aerodynamic Models

The aerodynamics model for non-hypersonic speeds operates from M = 0 into to the hypersonic range.[7]

The dynamic pressure is

$$q = \frac{1}{2}\rho u^2 \tag{1}$$

where u is the velocity and ρ is the density. The Reynold's number is

$$R_E = \frac{ul}{\nu} \tag{2}$$

where l is the representative length and ν is the kinematic viscosity.

We break the model into three regions

$$M = 0 \tag{3}$$

$$0 \leq M < 1 \tag{4}$$

and

$$M \geq 1 \tag{5}$$

The three drag components are the skin friction C_{D_s}, the form drag C_{D_f} and the parasitic drag,

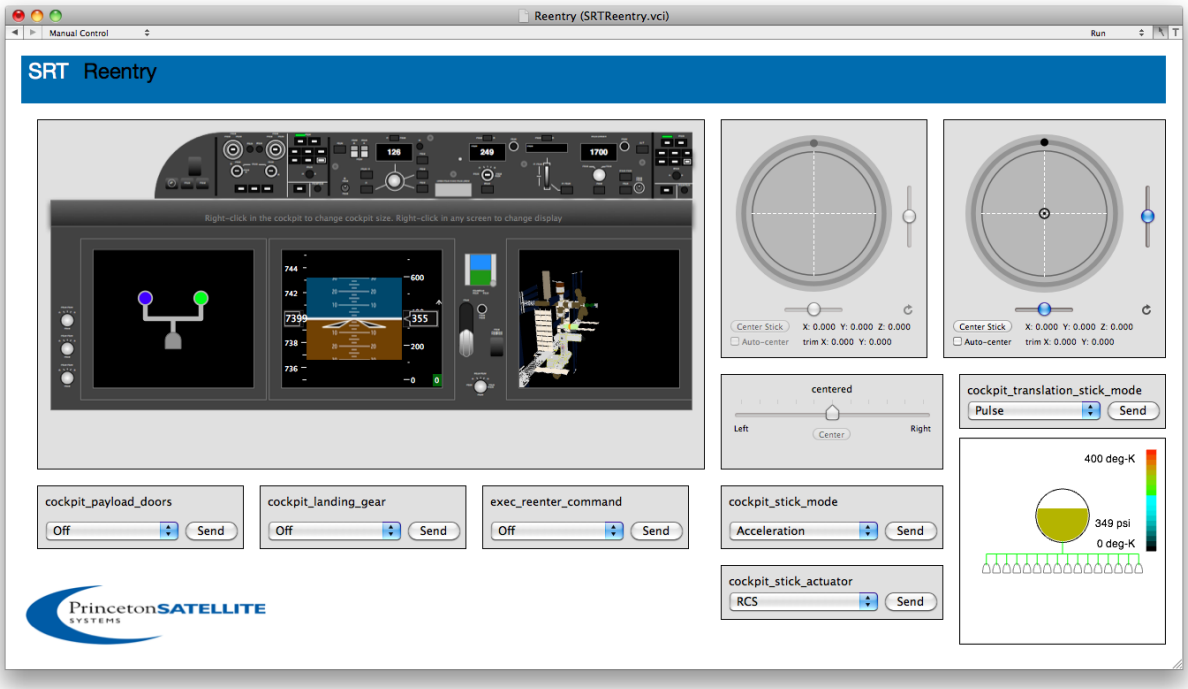

Figure 11: **Upper Stage Cockpit. The control can be operated in the simulation using the computers' mouse.**

C_{D_p} . For $M = 0$

$$C_{D_s} = 0 \tag{6}$$

$$C_{D_f} = 0 \tag{7}$$

$$k = \frac{1}{\eta_o \pi A} \tag{8}$$

where k is the induced drag constant, η_o is the Oswald efficiency factor and A is the aspect ratio For the subsonic regime

$$C_{D_s} = \frac{3}{4}\frac{1}{R_E^{1/5}} \tag{9}$$

$$C_{D_f} = \frac{1}{4}C_{D_s} \tag{10}$$

$$k = \frac{1}{\eta_o \pi A} \tag{11}$$

For the supersonic regime

$$C_{D_s} = \frac{3}{4}\frac{1}{\sqrt{M}R_E^{1/5}} \tag{12}$$

$$f = \sqrt{M^2 + 2\zeta M - 1} \tag{13}$$

$$C_{D_f} = \frac{4t}{f} \tag{14}$$

$$k = \frac{1}{4}f \tag{15}$$

ζ is a damping factor to prevent infinite form drag at $M = 1$. t is the thickness of the wing.

The parasitic drag is

$$C_{D_p} = \frac{1}{10}(C_{D_s} + C_{D_f}) \tag{16}$$

The drag coefficient at zero lift is

$$C_{D_0} = C_{D_s} + C_{D_f} + C_{D_p} \tag{17}$$

The lift coefficient is

$$C_L = C_{L_0} + C_{L_\alpha}(\alpha - \alpha_0) \tag{18}$$

where α is angle of attack. The drag coefficient is

$$C_D = C_{D_0} + kC_L^2 \tag{19}$$

The drag is

$$D = sqC_D \tag{20}$$

where s is the surface area contributing to lift and drag. The wing loading is

$$W = qC_L \tag{21}$$

The lift is

$$L = sW \tag{22}$$

These forces are compute individually for each rotatable surface. This does not account for the interaction among surfaces. The force on each surface is

$$F_i = -Du_i + Ln_i \tag{23}$$

whre n_i is perpendicular to u_i in the xz-plane.

The torque on each plate is

$$T_i = (r_i - c) \times F_i \tag{24}$$

where c is the center of mass and r_i is the vector to the aerodynamic center.

At hypersonic speeds we use inviscid newtonian flow models (basic momentum transfer models).[8]

The angle of the plate to the flow is

$$\sin\theta = \frac{-\mathbf{v}_\infty \cdot \mathbf{n}}{v_\infty} \tag{25}$$

where v_∞ is the freestream velocity, $\mathbf{n}$ is the unit normal vector to the plate, and θ is the angle between a tangent to the surface and the normal vector, or the 3D angle of attack.

The pressure coefficient is then calculated for the plate:

$$C_{P_i} = c_{p_{\max}} \sin^2\theta \tag{26}$$

where $c_{p_{\max}}$ is

$$c_{p_{\max}} = \frac{p_{02} - p_\infty}{q} \tag{27}$$

and

$$\frac{p_{02}}{p_\infty} = \left[\frac{(\gamma-1)^2 M_\infty^2}{4\gamma M_\infty^2 - 2(\gamma-1)}\right]^{\frac{\gamma}{\gamma-1}} \times \left[\frac{1-\gamma+2\gamma M_\infty^2}{\gamma+1}\right] \tag{28}$$

In the case where the plate is facing away from the freestream velocity vector, $C_P = 0$. The force on each plate is computed

$$F_i = qC_{P_i}u_i \tag{29}$$

where u_i is the local velocity vector. The torque on each plate is

$$T_i = (r_i - c) \times F_i \tag{30}$$

where c is the center of mass. The Newtonian model uses a simplified plate model of the vehicle Figure 12. Shadowing of surfaces is not modeled.

The two models are combined using the logistic function

$$T = T_l(1-f) + T_n f \tag{31}$$

$$F = T_l(1-f) + F_n f \tag{32}$$

where the subscript l means low-speed and n means Newtonian. f is the logistic function and is

$$f = \frac{1}{1 - e^{-aM-b}} \tag{33}$$

where a and b are weights.

B. Reentry Guidance and Control for SRT

Introduction

Takeoff through ISS rendezvous was demonstrated in previous work.[6] This section presents new results on reentry trajectory design and control.

Reentry Guidance

Reentry guidance and control is similar to the Space Shuttle.[9]

The reentry trajectory is an analytical solution of simplified ballistic flight equations of motion:

$$\dot{V} = D - g\sin\gamma \tag{34}$$

$$V\dot{\gamma} = \left(\frac{V^2}{r} - g\right)\cos\gamma + L_V\cos\phi \tag{35}$$

$$V\cos\gamma\dot{\psi} = \frac{V^2}{r}\cos^2\gamma\sin\psi\tan\theta + L_V\sin\phi \tag{36}$$

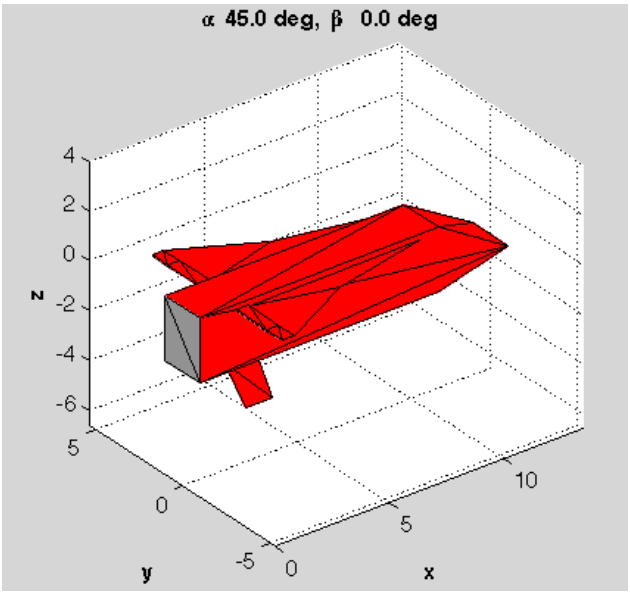

Figure 12: **Upper Stage simplified panel model**

where γ is the flight path angle, ϕ is the bank angle, θ is the latitude, and ψ is the azimuth of the velocity vector.

The trajectory is constructed to target a final altitude and velocity. The primary kinematic control is the flight path angle, which is effectively controlled by modulating the bank angle with a constant angle of attack. The nominal trajectory satisfies constraints on maximum acceleration, heating rate and dynamic pressure. Following the methodology of Harpold and Graves,[9] four phases of reentry are defined and combined to form the nominal trajectory. In each of the phases, a commanded drag function is defined as a function of Earth-relative velocity. Figure 13 shows the nominal trajectory as in terms of the drag vs. velocity, while Figure 14 shows the lift over drag profile that generates the nominal trajectory.

1. Quadratic drag acceleration

$$D = c_1 + c_2 V + c_3 V^2 \tag{37}$$

2. Equilibrium glide

$$D = \frac{g}{L/D}\left(1 - \frac{V^2}{V_s^2}\right) \tag{38}$$

3. Constant drag

$$D = c_4 \tag{39}$$

4. Transition

$$D = D_f + c_5\left(E - E_f\right) \tag{40}$$

where c_1 through c_3 are free parameters to shape the function, V_s is a arbitrary reference velocity, and E is the energy of the trajectory. The parameters c_4, c_5 and V_s are solved for to complete a continuous trajectory.

The nominal trajectory has a range of 6,400 km from the point where the Earth's atmosphere is penetrated. To accommodate ranges that vary from the nominal, the magnitude of the function can be varied while the shape is maintained. Each phase of the trajectory has an analytical

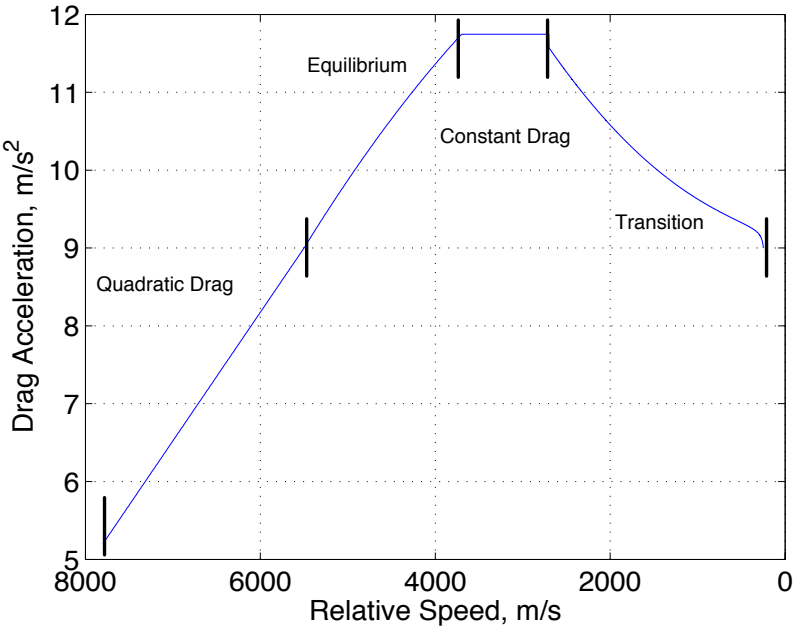

Figure 13: **SRT nominal reentry trajectory.**

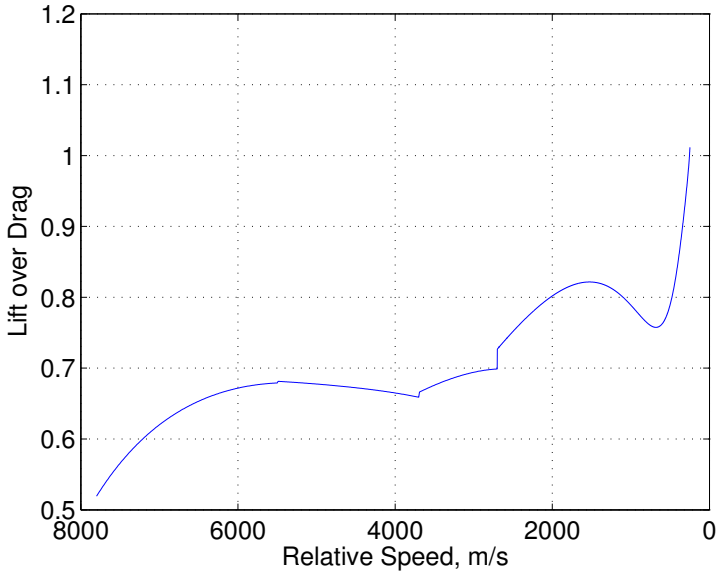

Figure 14: **Reentry lift over drag profile.**

solution for the range as follows:

if $Q > 0$

$$\begin{aligned} r_1 &= \frac{-1}{2c_3}\log\left(\frac{c_1+c_2V_f+c_3V_f}{c_1+c_2V+c_3V}\right) \\ &\quad +\frac{c_2}{c_3\sqrt{Q}}\tan^{-1}\left(\frac{2c_3V_f+c_2}{\sqrt{Q}}\right) \\ &\quad -\frac{c_2}{c_3\sqrt{Q}}\tan^{-1}\left(\frac{2c_3V_+c_2}{\sqrt{Q}}\right) \end{aligned} \quad (41)$$

if $Q < 0$

$$\begin{aligned} r_1 &= \frac{-1}{2c_3}\log\left(\frac{c_1+c_2V_f+c_3V_f}{c_1+c_2V+c_3V}\right) \\ &\quad +\frac{c_2}{2c_3\sqrt{-Q}}\log\left(\frac{A}{B}\right) \end{aligned} \quad (42)$$

where $Q = 4c_3c_1 - c_2^2$,

$$A = \frac{2c_3V_f + c_2 - \sqrt{-Q}}{2c_3V_f + c_2 + \sqrt{-Q}}$$

and

$$B = \frac{2c_3V + c_2 - \sqrt{-Q}}{2c_3V + c_2 + \sqrt{-Q}}.$$

$$r_2 = \frac{1}{2}\left[\left(\frac{V_s^2 - V^2}{D}\right)\log\left(\frac{V_f^2 - V_s^2}{V^2 - V_s^2}\right)\right] \quad (43)$$

$$r_3 = \frac{V^2 - V_f^2}{2c_4} \quad (44)$$

$$r_4 = \frac{E - E_f}{D - D_f}\log\left(\frac{D}{D_f}\right) \quad (45)$$

Eq. (41) through Eq. (45) can be used to compute free variables to satisfy a given range throughout the evolution of the trajectory. Following this methodology, the trajectory can be adjusted off the nominal so that accelerations are found that adjust for errors in the model as the orbiter progresses towards landing.

Reentry Control

The reentry control system tracks the gradually changing L/D profile described above, which varies as a function of Earth-relative velocity. To do so, the vehicle maintains a constant angle of attack and controls L/D through bank angle modulation. The L/D characteristics of the SRT in the hypersonic regime are approximated by evaluating the summation of Newtonian flow effects from the flat plates that comprise the CAD model. The current model exhibits a maximum L/D of about 1.5 at $\alpha = 35$ deg. By rotating the lift vector through the bank angle, the L/D may be reduced to reach the target value in the reentry profile. Periodic switching of the bank angle from one side to the other is required to prevent excessive cross-track drift.

Reentry begins by firing the RCS thrusters in the anti-velocity direction until the orbit perigee drops below 100 km. The main engine is not used in order to reduce the number of restarts, which extends the effective life of the engine. From a 350 km altitude orbit the deorbit burn with the RCS takes approximately 800 seconds. Next, the SRT reorients to align its nose forward, with wings level and a 35 deg angle of attack for maximum lift-to-drag. While still in the exoatmospheric regime, the RCS is used to maintain the desired attitude. At approximately 90 km, the dynamic pressure grows above 0.2 PSF and a blend of RCS and control surfaces is used.

Along the nominal reentry profile, the open-loop dynamics of the vehicle are evaluated to develop a series of linear models for control synthesis. Point controllers are designed to track bank angle and angle-of-attack reference commands using symmetric pairs of ailerons, elevators, and stabilators. Blending of the RCS is accomplished by incorporating its effect as a known disturbance torque input to the control system. The percentage of torque provided by the RCS is diminished as the dynamic pressure increases. The development of this integrated control system is ongoing and results will be presented in future publications.

Figure 15 illustrates the SRT simulation running in VisualCommander. Following completion of the de-orbit burn and attitude maneuver, the SRT is at 150 km altitude and approaching the atmospheric reentry starting conditions.

Manual Control Near ISS

Manual control is demonstrated with a y-axis burn to separate from the ISS. Manual thruster control passes rotation and translation demands to a simplex solver for thruster allocation.

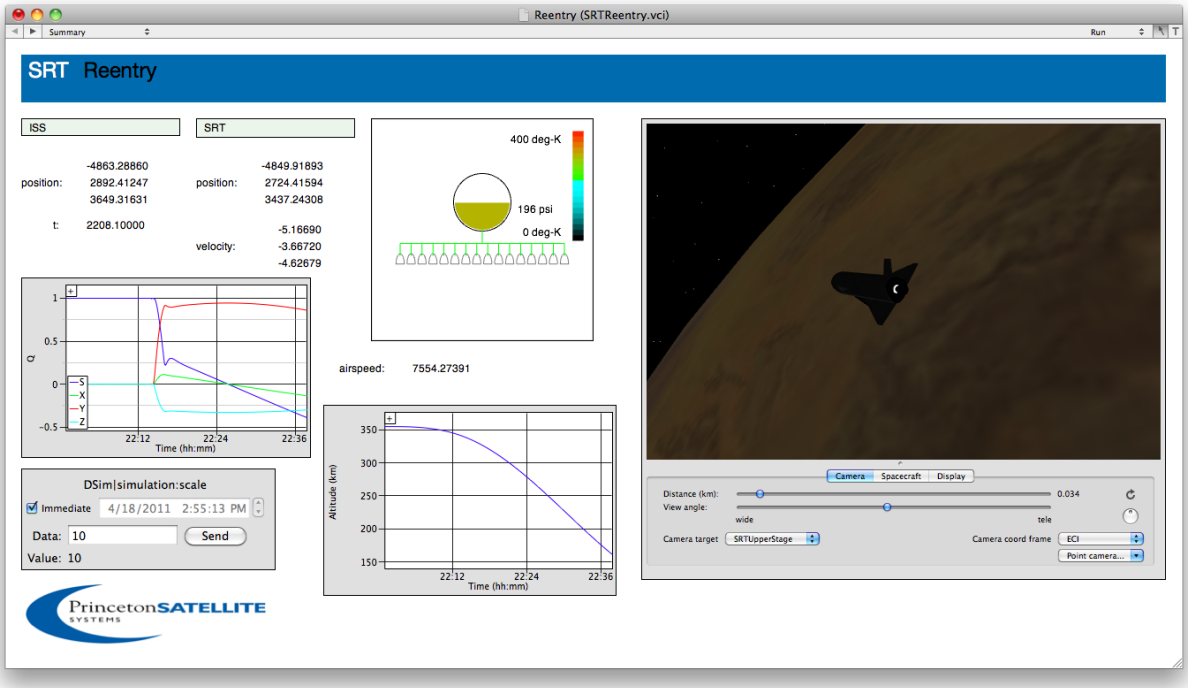

Figure 15: **SRT Following Reentry Profile at 150 km.**

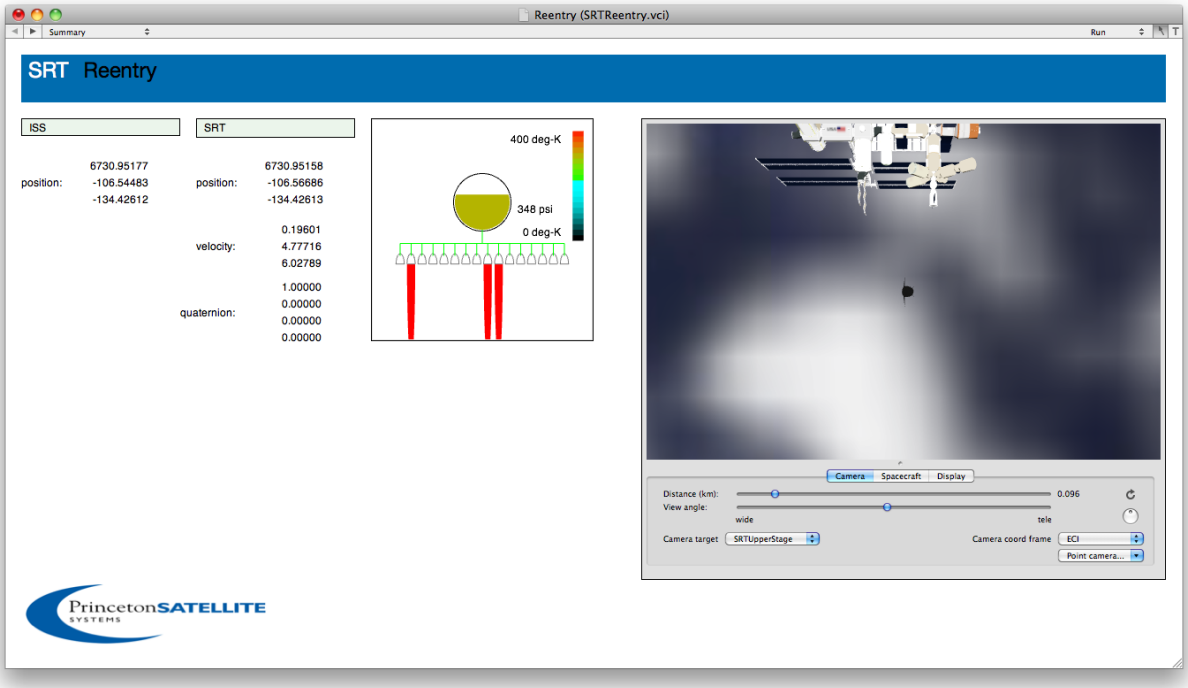

Figure 16: **Manual departure from ISS.**

Conclusions

This paper presents an overview of the design for the Space Rapid Transit launch vehicle. Elements of the mechanical design and group mass statements are presented, along with details of the simulation models, GN&C algorithms, and prototype flight software.

Development of the SRT is ongoing. Completion of the closed loop simulation that is discussed in this paper will enable PSS engineers to further optimize the vehicle design and mass budgets. At this point, all relevant GN&C algorithms will be implemented, and the performance of the vehicle can be tested through simulation throughout its mission profile.

The SRT shows that it is possible to assemble a high performance launch vehicle to meet the responsive needs of the nation's armed forces without relying on exotic technology. Not only is the timeframe of the development plan shortened with this strategy, but the cost and risks are significantly reduced. SRT can provide truly responsive space access in the near term.

References

[1]Griesemer, P. R., Mueller, J. B., Paluszek, M. A., and Du, J., "System Design of a Reusable, Horizontal Take-Off/Horizontal Landing Two Stage to Orbit Vehicle," *46th AIAA/ASME/SAE/ASEE Joint Propulsion Conference*, Nashville, TN, July 2010.

[2]"RL-10," Aerospace Guide, `http://www.aerospaceguide.net/rocketengines/RL10B-2.html`.

[3]Pichon, T., Lacombe, A., Joyez, P., Ellis, R., Humbert, S., and Payne, F. M., "RL10B-2 - Nozzle Extension Assembly Improvements for Delta IV," , No. AIAA-2001-3549.

[4]"RL-10 - Specifications," Space and Tech, `http://www.spaceandtech.com/spacedata/engines/rl10_specs.shtml`.

[5]Neff, K., King, P., Anflo, K., and Mollerberg, R., "High Performance Green Propellant for Satellite Applications," , No. AIAA 2009-4878.

[6]Mueller, J. B., Griesemer, P. R., Paluszek, M. A., and Du, J., "Unified GN&C System for the Space Rapid Transit Launch Vehicle," *AIAA GN&C Conference*, August 2010.

[7]Miller, R., *16.751 Notes*, MIT Aeronautics and Astronautics, 1977.

[8]Anderson, J. D., *Hypersonic and High-Temperature Gas Dynamics*, AIAA, 2nd ed., 2006.

[9]Harpold, J. and Graves, C., "Shuttle Entry Guidance," Tech. Rep. NASA-TM-79949, NASA Johnson Space Center, February 1979.